JOURNAL OF CATALYSIS **170,** 191–199 (1997)
ARTICLE NO. CA971752

# Supported Au Catalysts Prepared from Au Phosphine Complexes and As-Precipitated Metal Hydroxides: Characterization and Low-Temperature CO Oxidation

Youzhu Yuan,*,† Anguelina P. Kozlova,* Kiyotaka Asakura,‡ Huilin Wan,† Khirui Tsai,†
and Yasuhiro Iwasawa*,[1]

*Department of Chemistry, Graduate School of Science, The University of Tokyo, Hongo, Bunkyo-ku, Tokyo 113, Japan; †Department of Chemistry and the State Key Laboratory of Physical Chemistry for Solid Surface, Xiamen University, Xiamen 361005, China; and ‡Research Center for Spectrochemistry, Faculty of Science, The University of Tokyo, Hongo, Bunkyo-ku, Tokyo 113, Japan

Received January 23, 1997; revised May 13, 1997; accepted May 14, 1997

**Supported Au catalysts were prepared by attaching Au phosphine complexes, $Au(PPh_3)(NO_3)$ (1) and $[Au_9(PPh_3)_8](NO_3)_3$ (2), on as-precipitated metal hydroxides $M(OH)_x^*$ (*, as-precipitated; $M = Mn^{2+}$, $Co^{2+}$, $Fe^{3+}$, $Ni^{2+}$, $Zn^{2+}$, $Mg^{2+}$, $Cu^{2+}$, $Ti^{4+}$, $Ce^{4+}$, and $La^{3+}$), followed by temperature-programmed calcination in a flow of dry air. The obtained Au catalysts showed high catalytic activities in low-temperature CO oxidation. Among the obtained Au catalysts 1/$Mn(OH)_2^*$ and 1/$Co(OH)_2^*$ were most highly active even at 203 K. 1/$Fe(OH)_3^*$ and 1/$Ti(OH)_4^*$ also catalyzed CO oxidation at low temperatures 203–273 K, whereas 1/$Fe_2O_3$ and 1/$TiO_2$ prepared by supporting 1 on conventional $Fe_2O_3$ and $TiO_2$ showed negligible activity under the similar reaction conditions. It was estimated by TEM and XRD that the mean diameter of Au particles in 1/$Fe(OH)_3^*$ was about 2.9 nm, which was about 10 times smaller than that for 1/$Fe_2O_3$. EXAFS for 1/$Ti(OH)_4^*$ revealed that the coordination number of Au–Au bond was 8–10, while that for 1/$TiO_2$ was 11.0, which also indicates that Au particle size for 1/$Ti(OH)_4^*$ is smaller than that for 1/$TiO_2$. The catalysts obtained by attaching the Au complexes on commercially available metal hydroxides also showed negligible activity for the low-temperature CO oxidation under identical conditions. These results demonstrate that supported Au catalysts with small Au particles, tremendously active for the low-temperature CO oxidation, can be prepared by attaching the Au phosphine complexes on the as-precipitated metal hydroxides. Sodium cations exhibited positive effect on the Au catalysis, whereas chloride anions drastically decreased the CO oxidation activity.** © 1997 Academic Press

## INTRODUCTION

Low-temperature CO oxidation has been extensively studied as the key issue relevant to gas purification in $CO_2$ lasers, CO gas sensors, air-purification devices for respiratory protection, and pollution control devices for reducing industrial and environmental emission and removing a trace quantity of CO from the ambient air in enclosed atmospheres such as submarines and space crafts on long-duration missions (1–27). Although Pt/$SnO_x$ and Pd/$SnO_x$ are effective catalysts for this reaction (1–3), there are complications of pretreatments for catalyst reduction and induction periods before reaching maximum catalytic activities (4). It has been reported that Au particles dispersed on oxide supports are active for catalytic CO oxidation (5–7). Haruta and co-workers screened a number of reducible-oxide-supported metals and found that small Au particles supported on $\alpha$-$Fe_2O_3$, $Co_3O_4$, $TiO_2$, *and* NiO were efficient CO oxidation catalysts at low temperatures (8–13). Hoflund and co-workers also demonstrated that Au on $MnO_x$ was active for this reaction (18, 19). Numerous experimental results have demonstrated that supported Au particles work as CO oxidation catalysts (20–25).

Support effect and particle size effect on the Au catalysis have been substantiated with a number of Au catalysts. Au/$Fe_2O_3$, Au/$Co_3O_4$, Au/NiO, Au/$Al_2O_3$, and Au/$SiO_2$ showed an overall trend that the CO oxidation activity increased with decreasing size of the Au particles (9). Ultrafine Au particles may be prerequisite for observation of a Au–support interaction (26). Given this assumption, the reactivity of supported Au catalysts may be determined by the method of catalyst preparation which controls Au particle size and Au–support interaction.

Use of molecular metal complexes is a promising way to prepare tailored metal catalysts with more efficient interaction between metal and support to generate unique catalysis (27–32). However, it is scarcely reported that supported Au catalysts with small particles are obtained by decomposition of Au complexes or Au clusters. Our earlier work (33, 34) showed that phosphine-stabilized Au complexes and clusters supported on inorganic oxides were readily decomposed to form gold metallic particles by heat treatments in vacuum and the obtained catalysts were active for CO oxidation under mild conditions, typically at 300–400 K. XRD

---

[1] To whom all correspondence should be addressed. Fax: 81-3-5800-6892. E-mail: iwasawa@utsc.s.u-tokyo.ac.jp.

0021-9517/97 $25.00

and EXAFS revealed that Au particles with sizes >12 nm were formed on the oxide surfaces by the heat treatment.

Recently, we developed a new way to prepare supported Au catalysts with highly dispersed Au particles by attaching a Au phosphine complex $Au(PPh_3)(NO_3)$ (**1**) and a Au phosphine cluster $[Au_9(PPh_3)_8](NO_3)_3$ (**2**), on as-precipitated metal hydroxides, followed by temperature-programmed calcination in a flow of air (35). The highly dispersed Au particles on the specially obtained supports showed extremely high activity for catalytic CO oxidation at low temperatures. Here we report the characterization by EXAFS, XRD, and TEM and performance for low-temperature CO oxidation of the Au catalysts prepared from the Au complexes **1** or **2** and the as-precipitated metal hydroxides.

## EXPERIMENTAL

### *Preparation of Catalyst*

Au phosphine complex, $Au(PPh_3)(NO_3)$ (**1**), and Au phosphine cluster, $[Au_9(PPh_3)_8](NO_3)_3$ (**2**) were synthesized according to the literature (36, 37). As-precipitated metal hydroxides were prepared by precipitation of metal nitrates (99.9% purity) with an aqueous solution of $Na_2CO_3$ (99.9%) in a similar manner to the coprecipitation method (9–14). As-precipitated vanadium hydroxide was obtained by hydrolysis of vanadium chloride (99.9%) with an aqueous solution of $Na_2CO_3$. The precipitates were repeatedly washed until no Cl was detected in the filtrates. Three kinds of as-precipitated $Ti(OH)_4^*$ were obtained by hydrolysis of $Ti(i\text{-}OC_3H_7)_4$ (titanium-tetra-*iso*-propoxide, 99.999%) with deionized water (denoted as W-$Ti(OH)_4^*$), by hydrolysis with an aqueous solution of $Na_2CO_3$ (denoted as S-$Ti(OH)_4^*$), and by hydrolysis with deionized water, followed by impregnation of $Na_2CO_3$ (Na/Au = 1.0 in an atomic ratio) (denoted as D-$Ti(OH)_4^*$). The precipitates were repeatedly washed with deionized water until the pH became 7.0. The as-precipitated $M(OH)_x^*$ were filtered and immediately impregnated with an acetone (99.9%) solution of **1** or a methanol (99.8%) solution of **2**, with vigorous stirring for at least 12 h, followed by evacuation for 5 h to remove the solvent at room temperature. The obtained samples were calcined in a glass tube at a heating rate of 4 K/min to 673 K and at 673 K for 4 h in a flow of air (30 ml/min). The catalysts thus prepared are denoted as **1**/$M(OH)_x^*$ or **2**/$M(OH)_x^*$. Note that the samples are always used as catalysts after the temperature-programmed calcination. For comparison, Au/$Fe_2O_3$ catalysts were prepared by a coprecipitation method by using $HAuCl_4$ and $Fe(NO_3)_3$ as reported in literature (9, 10) and by impregnating **1** or **2** on commercially available $Fe_2O_3$ and $TiO_2$ (Desussa P-25). These catalysts are denoted as coprec-Au/$Fe_2O_3$ and **1** or **2**/$Fe_2O_3$ and **1** or **2**/$TiO_2$. The impregnated samples were calcined in the similar way to that for **1** or **2**/$M(OH)_x^*$. The Au loading on each support was controlled to be 3.0 wt% except for the coprecipitated catalyst (10 wt%).

### *Characterization*

The samples were characterized by X-ray diffraction (XRD), Transmission electron microscopy (TEM), and extended X-ray absorption fine structure (EXAFS). XRD patterns were recorded on a Rigaku powder X-ray diffractometer with Cu$K\alpha$ radiation over the $2\theta$ range 20°–80°. The TEM image for the Au catalysts was observed using a Hitachi H-1500 electron microscope operated at 800 kV. At least 300 particles were used to determine the mean diameter of Au particles. Au $L_3$-edge EXAFS spectra were measured in a transmission mode at BL-10B of the Photon Factory in the National Laboratory for High Energy Physics (Proposal No. 95G200). The measurements were carried out at a beam current of 250–350 mA and a storage-ring energy of 2.5 GeV. The samples were calcined in a U-shaped glass tube combined in a fixed-bed flow reaction system in a flow of air (30 ml/min) and transferred to EXAFS cells connected to the U-shaped glass tube. Data were analyzed by a curve-fitting method, using empirically derived phase-shift and amplitude functions. The interactions of Au–Au and Au–P were calculated by using the FEFF6.0 software (38, 39). The parameters used for the analysis are summarized in Table 1.

### *Catalytic CO Oxidation*

CO oxidation reactions were carried out in a fixed-bed flow reactor equipped with a computer-controlled auto-sampling system by using 200 mg catalyst powder. The reaction gas containing 1.0% CO balanced with air purified through a molecular sieve column was passed through the catalyst bed at a flowrate of 67 ml/min (SV = 20,000 ml/h/g). Reaction products were analyzed by a gas chromatograph using a column of Unibeads C for $CO_2$ and a column of 5A molecular sieve for CO and $O_2$. The material balance in the

**TABLE 1**

**Crystallographic Data for FEFF Calculation and Fourier Transform Ranges Used in the EXAFS Analysis**

| FEFF calculation | | | Fourier range | |
|---|---|---|---|---|
| Shell | $N$ | $r$ (Å) | $\Delta k$ range (Å$^{-1}$) | $\Delta r$ range (Å) |
| Au–P for $Au(PPh_3)$ | 1.0 | 2.28 | 3.0–14.50 | 1.40–2.30 |
| Au–Au for Au(Au) or Au(Pt) | 1.0 | 2.87 | 3.0–14.50 | 2.00–3.20 |
| Au–Au for Au foil | 1.0 | 2.87 | 3.0–16.0 | 2.10–3.15 |

*Note.* $N$, coordination number of backscatterer; $r$, distance; $\Delta k$, range used for Fourier transformation ($k$, wave number); $\Delta r$, range used for Fourier filtering ($r$, distance).

catalytic reactions was checked from the concentration of $CO_2$ and CO, showing good balance under all the reaction conditions examined.

## RESULTS

### *Characterization of EXAFS, XRD, and TEM*

EXAFS measurements in a transmission mode have been carried out at room temperature to characterize **1**/$TiO_2$ and **1**/$Ti(OH)_4^*$. The Fourier transforms of EXAFS oscillations at Au $L_3$-edge for **1**/$TiO_2$ and **1**/$Ti(OH)_4^*$, before and after calcination are shown in Fig. 1. The peaks around 1.8 Å in Figs. 1a, 1b, and 1c are assignable to Au–P bond, which indicates that upon supporting the Au phosphine complex **1** on W-$Ti(OH)_4^*$, S-$Ti(OH)_4^*$, and $TiO_2$ the complex **1** is not decomposed. However, after calcination at 673 K in air, the EXFAS Fourier transform peak shifted to longer distance. The EXAFS curve-fitting analysis revealed that the new peak is due to Au–Au bonding. The coordination number and distance of Au–Au bond were determined to be 8.3 and 2.86 Å for **1**/W-$Ti(OH)_4^*$ and 9.8 and 2.86 Å for **1**/S-$Ti(OH)_4^*$, while those for **1**/$TiO_2$ were 11.0 and 2.87 Å, as shown in Table 2. No Au–P bond was observed with the calcined samples. The results demonstrate that the Au complexes on the supports were decomposed to form metallic Au particles by the calcination at 673 K. The coordination numbers for **1**/$Ti(OH)_4^*$ and **1**/$TiO_2$ were different from each other, suggesting the formation of Au particles with different sizes.

The change in the Au species from the phosphine complex to metallic particles was accompanied by the development of the XRD peaks for crystalline $TiO_2$ as shown in Fig. 2. The peaks for $TiO_2$ derived from $Ti(OH)_4^*$ are much broader than those for $TiO_2$ (P-25). When S-$Ti(OH)_4^*$ obtained by hydrolysis of Ti(*i*-$OC_3H_7$)$_4$ with an aqueous solution of $Na_2CO_3$ was used as a support for **1**, the calcined sample **1**/S-$Ti(OH)_4^*$ constituted an amorphous type of $TiO_2$ (Fig. 2d). Contrary to this, when Ti(*i*-$OC_3H_7$)$_4$ was hydrolyzed by $H_2O$, the $TiO_2$ structure in **1**/W-$Ti(OH)_4^*$ was mainly of anatase type (Fig. 2b). The **1**/$TiO_2$ catalyst showed a Au(200) peak at $2\theta = 44.4^\circ$, whereas the XRD peak for crystalline Au particles was hardly observed with **1**/W-$Ti(OH)_4^*$, **1**/D-$Ti(OH)_4^*$, and **1**/S-$Ti(OH)_4^*$ as shown in Figs. 2b–2d.

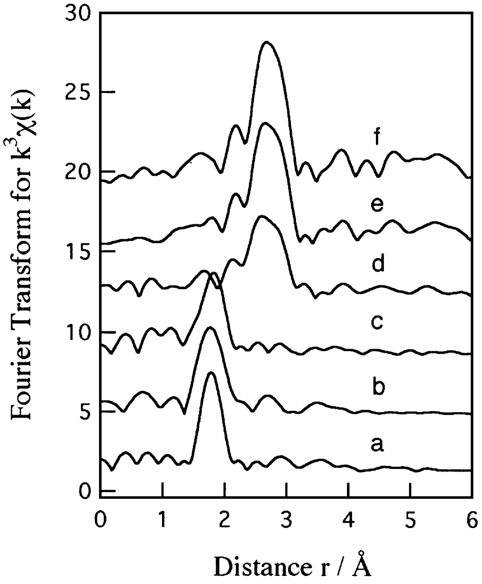

**FIG. 1.** Fourier transforms of EXAFS oscillation at Au $L_3$-edge for **1**/$TiO_2$ and **1**/$Ti(OH)_4^*$, before and after calcination. (a) **1**/W-$Ti(OH)_4^*$ (before calcination); (b) **1**/S-$Ti(OH)_4^*$ (before calcination); (c) **1**/$TiO_2$ (before calcination); (d) **1**/W-$Ti(OH)_4^*$ (after the temperature-programmed calcination); (e) **1**/S-$Ti(OH)_4^*$ (after the temperature-programmed calcination); (f) **1**/$TiO_2$ (after the temperature-programmed calcination).

Figure 3 shows the XRD patterns for the Au/Fe oxide catalysts, coprec-Au/$Fe_2O_3$, **1**/$Fe_2O_3$, **1**/$Fe(OH)_3^*$, **2**/$Fe(OH)_3^*$, $Au(PPh_3)Cl/Fe(OH)_3^*$, $HAuCl_4/Fe(OH)_3^*$, and calcined $Fe(OH)_3^*$. The intensity of the diffraction peak at $2\theta = 38.2^\circ$

**TABLE 2**

**Curve-Fitting Results for the Au $L_3$-Edge EXAFS Data of 1/$(TiOH)_4^*$ and 1/$TiO_2$**

| | Au–P | | | | Au–Au | | | | |
|---|---|---|---|---|---|---|---|---|---|
| *T* (K) | *N* | *r* (Å) | $\Delta\sigma^2$ (Å$^2$) | $\Delta E$ (eV) | *N* | *r* (Å) | $\Delta\sigma^2$ (Å$^2$) | $\Delta E$ (eV) | $R_f$ (%) |
| | | | | **1**/W-$(TiOH)_4^*$ | | | | | |
| 293 | 1.1 ± 0.2 | 2.20 ± 0.01 | 0.0021 | −5.42 | — | — | — | — | 1.7 |
| 673 | — | — | — | — | 8.3 ± 1.0 | 2.86 ± 0.01 | 0.0014 | 1.45 | 1.2 |
| | | | | **1**/S-$(TiOH)_4^*$ | | | | | |
| 293 | 1.4 ± 0.3 | 2.20 ± 0.01 | 0.0006 | −3.46 | — | — | — | — | 1.3 |
| 673 | — | — | — | — | 9.8 ± 1.0 | 2.86 ± 0.01 | 0.0001 | 2.55 | 0.9 |
| | | | | **1**/$TiO_2$ | | | | | |
| 293 | 1.3 ± 0.3 | 2.22 ± 0.01 | 0.0000 | −4.05 | — | — | — | — | 0.9 |
| 673 | — | — | — | — | 11.0 ± 1.0 | 2.87 ± 0.01 | 0.0001 | 2.12 | 0.7 |

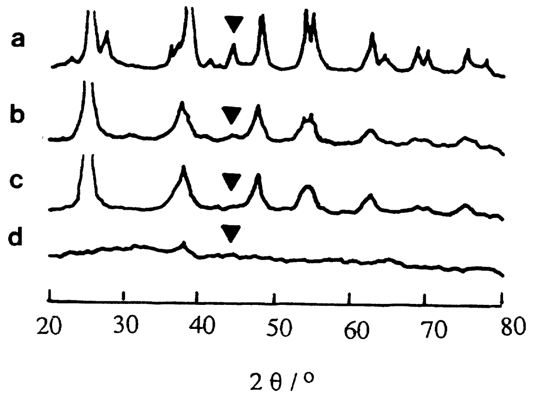

**FIG. 2.** XRD patterns of **1**/Ti(OH)$_4^*$ and **1**/TiO$_2$. ▼ indicates Au(200) peak. All the catalysts (hereinafter otherwise noted) are the ones after the temperature-programmed calcination. Catalysts: (a) **1**/TiO$_2$; (b) **1**/W-Ti(OH)$_4^*$; (c) **1**/D-Ti(OH)$_4^*$; (d) **1**/S-Ti(OH)$_4^*$.

for Au(111) depended on the kind of samples. The order of the sharpness of the Au(111) diffraction peak for the samples was as follows: Au(PPh$_3$)Cl/Fe(OH)$_3^*$ $>$ HAuCl$_4$/Fe(OH)$_3^*$ $\geq$ **2**/Fe(OH)$_3^*$ $\geq$ **1**/Fe$_2$O$_3$ $\gg$ coprec-Au/Fe$_2$O$_3$ $\geq$ **1**/Fe(OH)$_3^*$.

The Au particle sizes for **1**/Fe(OH)$_3^*$ and **1**/Fe$_2$O$_3$ were estimated by transmission electron micrograph in Fig. 4. The mean diameter of Au particles in **1**/Fe(OH)$_3^*$ was about 2.9 nm, where most of the particles ranged about 1–5 nm. In contrast, the mean diameter of Au particles in **1**/Fe$_2$O$_3$ was as large as 30 nm, ranging 10–50 nm. Thus much smaller Au particles are produced on the as-precipitated Fe(OH)$_3^*$ than on Fe$_2$O$_3$, which coincides with the results of EXAFS and XRD.

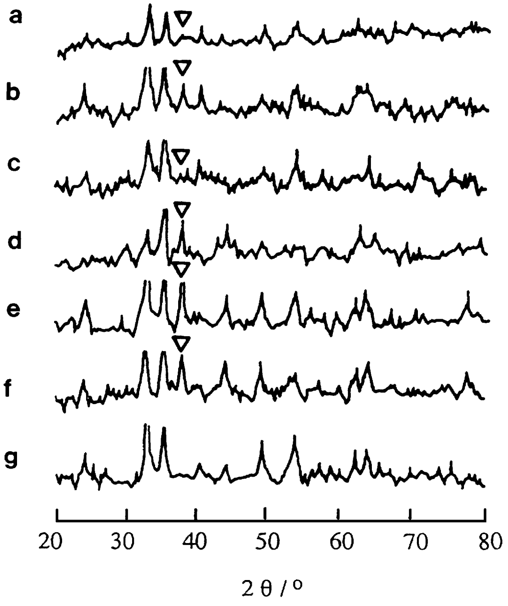

**FIG. 3.** XRD patterns of various Au/Fe oxide catalysts after the temperature-programmed calcination. ▽ indicates Au(111) peak. Catalysts: (a) coprec-Au/Fe$_2$O$_3$; (b) **1**/Fe$_2$O$_3$; (c) **1**/Fe(OH)$_3^*$; (d) **2**/Fe(OH)$_3^*$; (e) Au(PPh$_3$)Cl/Fe(OH)$_3^*$; (f) treated HAuCl$_4$/Fe(OH)$_3^*$; (g) Fe(OH)$_3^*$.

### *Catalytic Performance*

As a typical example, Fig. 5 depicts the catalytic activities (CO conversion) of the supported Au catalysts, coprec-Au/Fe$_2$O$_3$, **1**/Fe(OH)$_3^*$, **1**/Fe(OH)$_3^*$(dried), Fe(OH)$_3^*$ alone, and **1**/Fe$_2$O$_3$, for CO oxidation in a fixed-bed flow reactor as a function of reaction temperature. Under the present reaction condition (SV = 20,000 ml/h/g-cat; CO = 1%), 100% conversion corresponds to a reaction rate of $8.93 \times 10^{-3}$ mol/h/g-cat. It is to be noted that **1**/Fe(OH)$_3^*$ is tremendously active, compared with **1**/Fe$_2$O$_3$. The CO oxidation reaction on **1**/Fe$_2$O$_3$ proceeded only above 300 K, whereas the reaction on **1**/Fe(OH)$_3^*$ occurred even at 203 K. Under the present conditions the catalytic activity of the coprec-Au/Fe$_2$O$_3$ catalyst prepared by the coprecipitation method in the literature (9, 10) was much lower than that of the **1**/Fe(OH)$_3^*$ catalyst.

Table 3 shows comparison of the catalytic activities of various **1**/*M*(OH)$_x^*$ for CO oxidation. Among all the catalysts, those prepared by using the as-precipitated metal hydroxides originated from Mn(NO$_3$)$_2$, Co(NO$_3$)$_3$, Fe(NO$_3$)$_3$, Ni(NO$_3$)$_2$, Mg(NO$_3$)$_2$, Zn(NO$_3$)$_2$, and Ti(*i*-OC$_3$H$_7$)$_4$ were very active in CO oxidation at the low temperatures.

### *Influence of Sodium Cation*

The CO conversions on **1**/W-Ti(OH)$_4^*$(Na$^+$-free), **1**/S-Ti(OH)$_4^*$(containing Na$^+$), and **1**/D-Ti(OH)$_4^*$(Na$^+$-doped) are plotted as a function of reaction temperature in Fig. 6. It was found that **1**/S-Ti(OH)$_4^*$ was much more efficient for the low-temperature CO oxidation than **1**/W-Ti(OH)$_4^*$. Addition of a small amount of Na$^+$ ions to the

**TABLE 3**

**Catalytic CO Oxidation Activities of Various 1/*M*(OH)$_x^*$ Catalysts**

| Original catalyst | $T_s$ (K) | $T_{50\%}$ (K) | $T_{100\%}$ (K) |
|---|---|---|---|
| **1**/Mn(OH)$_2^*$ | <203 | <203 | 273 |
| **1**/Co(OH)$_2^*$ | <203 | <203 | 273 |
| **1**/Ni(OH)$_2^*$ | <203 | 230 | 273 |
| **1**/Fe(OH)$_3^*$ | <203 | 206 | 273 |
| **1**/Zn(OH)$_2^*$ | <203 | 248 | 273 |
| **1**/Ce(OH)$_4^*$ | 243 | 263 | 283 |
| **1**/Mg(OH)$_2^*$ | 203 | 250 | >373 |
| **1**/Ti(OH)$_4^*$ | 253 | 304 | 433 |
| **1**/Cu(OH)$_2^*$ | 223 | 334 | 443 |
| **1**/La(OH)$_3^*$ | 283 | 335 | 503 |
| **1**/Al(OH)$_3^*$ | 373 | 606 | >633 |
| **1**/V(OH)$_3^*$ | ~383 | 649 | >773 |
| **1**/Cr(OH)$_3^*$ | ~473 | 735 | >773 |

*Note.* $T_s$, temperature for CO oxidation to start; $T_{50\%}$, temperature for 50% conversion; $T_{100\%}$, temperature for 100% conversion.

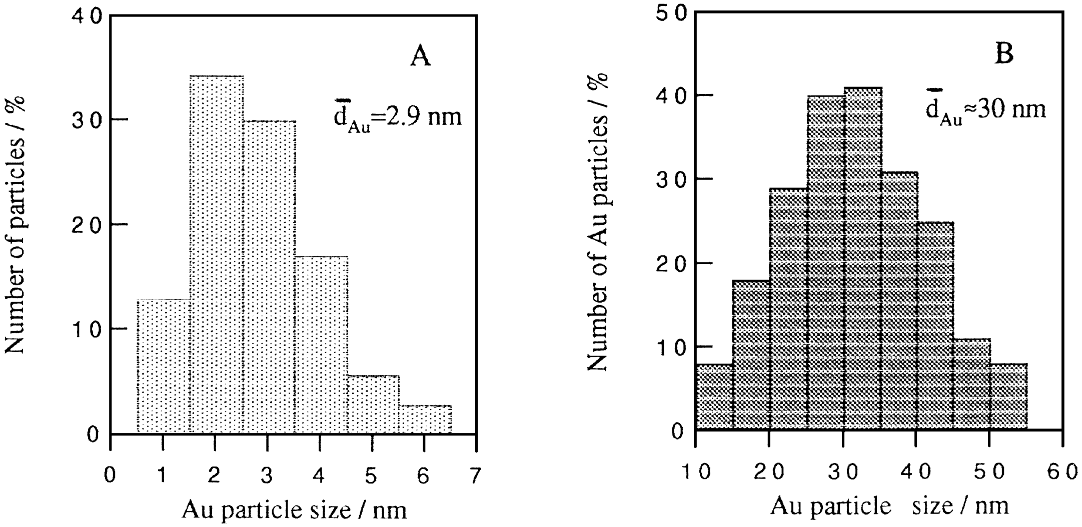

**FIG. 4.** Size distribution for Au particles estimated by TEM. Catalysts: (A) **1**/Fe(OH)$_3^*$; (B) **1**/Fe$_2$O$_3$.

as-precipitated W-Ti(OH)$_4^*$ by impregnation of aqueous Na$_2$CO$_3$ solution remarkably promoted the Au/Ti(OH)$_4^*$ catalysis.

Figure 7 shows the catalytic activities of **1**/S-Fe(OH)$_3^*$ which was derived from the as-precipitated Fe(OH)$_3^*$ prepared by using an aqueous solution of Na$_2$CO$_3$ and **1**/A-Fe(OH)$_3^*$ which was derived from the as-precipitated Fe(OH)$_3^*$ prepared by using an aqueous NH$_3$ solution under the identical pH condition. Although the remaining amount of sodium cation in the sample of **1**/S-Fe(OH)$_3^*$ has not been determined, it is evident that the coexistence of Na ions on the Fe(OH)$_3^*$ also has a positive effect on the CO oxidation catalysis of **1**/Fe(OH)$_3^*$.

### *Au Precursors*

The CO conversions over the catalysts, **1**/Fe(OH)$_3^*$, **2**/Fe(OH)$_3^*$, Au(PPh$_3$)Cl/Fe(OH)$_3^*$, HAuCl$_4$/Fe(OH)$_3^*$,

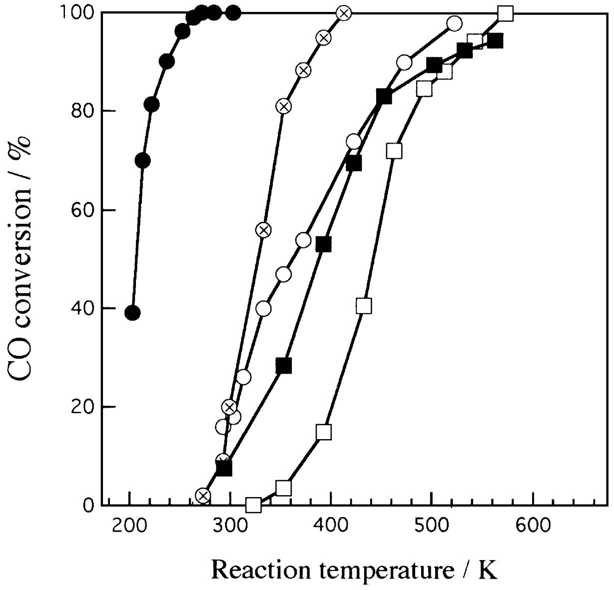

**FIG. 5.** Catalytic CO oxidation reactions on various Au/Fe oxide catalysts in a fixed-bed flow reactor (SV = 20,000 ml/h/g) as a function of reaction temperature. (●) **1**/Fe(OH)$_3^*$; (⊗) coprec-Au/Fe$_2$O$_3$; (○) **1**/dried Fe(OH)$_3^*$ (Fe(OH)$_3$ dried before supporting the Au complex); (■) **1**/Fe$_2$O$_3$; (□) Fe(OH)$_3^*$.

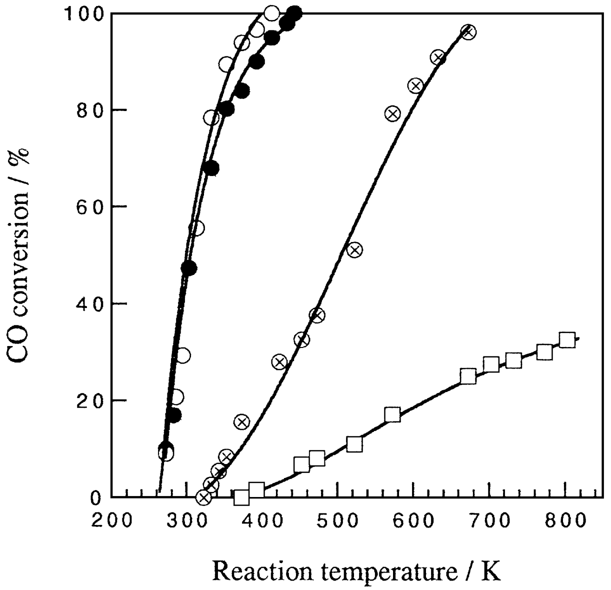

**FIG. 6.** Na effect on CO oxidation activity of the supported Au catalysts derived from different Ti(OH)$_4^*$ as a function of reaction temperature. (○) **1**/D-Ti(OH)$_4^*$; (●) **1**/S-Ti(OH)$_4^*$; (⊗) **1**/W-Ti(OH)$_4^*$; (□) W-Ti(OH)$_4^*$.

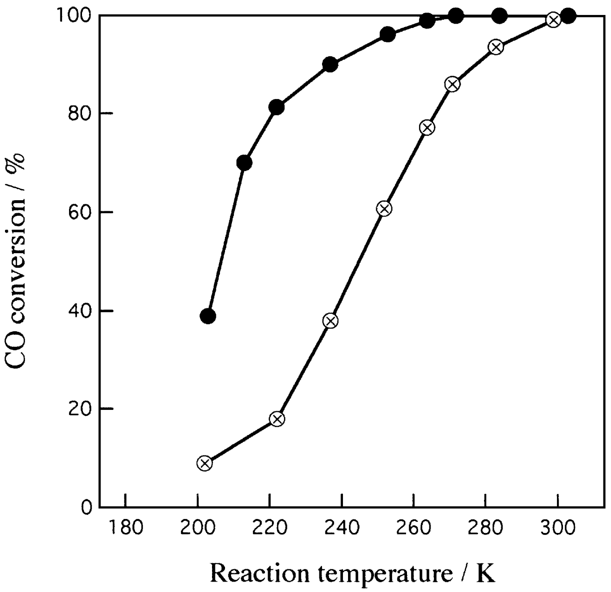

**FIG. 7.** Comparison of catalytic CO oxidation activities of two kinds of **1**/Fe(OH)$_3^*$. (●) Catalyst derived from Fe(OH)$_3^*$ precipitated by aqueous $Na_2CO_3$; (⊗) catalyst derived from Fe(OH)$_3^*$ precipitated by aqueous $NH_3$.

**1**/Mg(OH)$_2^*$, and **2**/Mg(OH)$_2^*$, in a fixed-bed flow reaction system are plotted against the reaction temperature in Fig. 8. The catalysts derived from **1** were superior to those derived from **2** for both Fe(OH)$_3^*$ and Mg(OH)$_2^*$. Moreover, when Au(PPh$_3$)Cl and HAuCl$_4$ were used as precursors, the obtained Au catalysts, Au(PPh$_3$)Cl/Fe(OH)$_3^*$ and HAuCl$_4$/Fe(OH)$_3^*$, showed much lower catalytic activities compared with **1** or **2**/Fe(OH)$_3^*$. The CO oxidation reaction on the Cl-containing precursor-derived catalysts proceeded only above 500 K (Fig. 8). These results may be attributed to poisoning by surface Cl ions which originate from the Au precursors and also to the larger Au particles in these catalysts as proved by XRD. The tremendous catalysis for low-temperature CO oxidation may be achieved by choosing the suitable Au precursors which is expected to interact with the as-precipitated hydroxide surfaces.

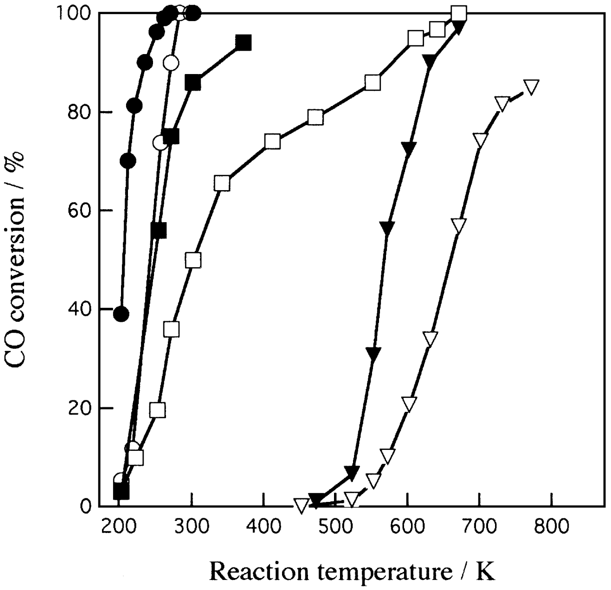

**FIG. 8.** CO oxidation activities of supported Au catalysts derived from different Au precursors as a function of reaction temperature. (●) **1**/Fe(OH)$_3^*$; (○) **2**/Fe(OH)$_3^*$; (■) **1**/Mg(OH)$_2^*$; (□) **2**/Mg(OH)$_2^*$; (▼) HAuCl$_4$/Fe(OH)$_3^*$; (▽) Au(PPh$_3$)Cl/Fe(OH)$_3^*$.

## DISCUSSION

It has been demonstrated that use of suitable metal complexes and clusters as precursors provides a promising way to prepare highly dispersed metal particles on oxide supports as well as unique structures with chemical bonding or interaction with oxide surfaces (32). To obtain highly dispersed Au particles on oxide surfaces, we chose phosphine-stabilized Au complex Au(PPh$_3$)(NO$_3$) (**1**) and Au cluster [Au$_9$(PPh$_3$)$_8$](NO$_3$)$_3$ (**2**) as precursors which could be thermally decomposed on the oxide surfaces. When the Au complexes (**1**) and (**2**) were supported on the metal oxides such as $Fe_2O_3$ and $TiO_2$, however, the supported Au complexes aggregated to large Au particles (about 30 nm in diameter) during the calcination at 673 K as characterized by EXAFS (coordination number of Au–Au bond) in Fig. 1 and Table 2, XRD in Figs. 2 and 3, and TEM in Fig. 4. These Au complex-derived Au particles on the traditional oxides showed low catalytic activities for the CO oxidation as typically depicted in Fig. 5. As the Au aggregation and low activity were thought to be due to almost no or weak interaction of the Au precursors with the oxide surfaces, the oxides were exposed to water vapor to produce surface OH groups for anchoring the Au complexes. The resultant Au complexes supported on the water vapor-treated oxides were easily decomposed to aggregate to large Au particles by calcination at 673 K. Next, metal hydroxides commercially available were used as the supports for the Au complexes, but the obtained supported Au catalysts also showed low activities.

We newly prepared the as-precipitated metal hydroxides $M$(OH)$_x^*$ by hydrolysis of various metal nitrates, vanadium chloride and titanium-tetra-isopropoxide with an aqueous solution of $Na_2CO_3$ (5 wt%). Then the Au complexes were attached on the wet $M$(OH)$_x^*$ followed by temperature-programmed (4 K/min) calcination up to 673 K in a flow of air as shown in Scheme 1. It was found that the obtained Au catalysts showed remarkably high catalytic activities for CO oxidation at low temperatures 200–273 K as shown in Figs. 5–8. It is evident from the results of EXAFS (Fig. 1), XRD (Figs. 2 and 3), and TEM (Fig. 4) that the

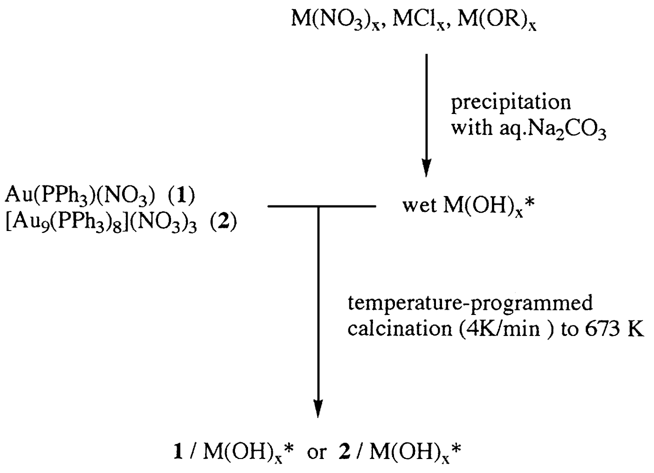

**SCHEME 1.** Preparation of the $\mathbf{1}/M(\mathrm{OH})_x^*$ or $\mathbf{2}/M(\mathrm{OH})_x^*$ catalysts.

Au particles in **1** or $\mathbf{2}/\mathrm{Ti(OH)}_4^*$ or $\mathrm{Fe(OH)}_3^*$ were several ten times smaller than those on the corresponding metal oxides, $TiO_2$ and $Fe_2O_3$. Negligible Au(200) and Au(111) peaks for $\mathbf{1}/\mathrm{Ti(OH)}_4^*$ (Fig. 2) and $\mathbf{1}/\mathrm{Fe(OH)}_3^*$ (Fig. 3), respectively, suggest that the diameter of the Au particles may be less than 3.0 nm, which coincides with the TEM data in Fig. 4. When the as-precipitated Fe hydroxide which was dried by evacuation at 473 K for 4 h was used as the support for **1**, the obtained $\mathbf{1}/\text{dry-}\mathrm{Fe(OH)}_3^*$ catalyst was much less active than the $\mathbf{1}/\mathrm{Fe(OH)}_3^*$, as shown in Fig. 5.

Our early works (32–34) demonstrate that the Au complexes **1** and **2** on the oxide supports readily decompose to metallic gold at lower temperatures than 573 K. In the similar temperature range the as-precipitated metal hydroxides are dehydrated to form anhydrous metal hydroxides and mostly to partially dehydrated metal oxides. The supported Au complexes are expected to be stabilized on the surface of the as-precipitated metal hydroxides by chemical interaction between $[\mathrm{Au(PPh_3)}]^+$ or $[\mathrm{Au_9(PPh_3)_8}]^{3+}$ and the hydroxyl groups of the as-precipitated metal hydroxide surfaces or water adsorbed on them. During calcination of the samples at 673 K the transformations of both Au complexes and as-precipitated hydroxides occur in parallel, which leads to the formation of highly dispersed Au particles on the *in situ* prepared oxide surfaces. On the other hand, in the case of Au complex/$M_x\mathrm{O}_y$, there is only a limited number of OH groups on the oxide surface and the interaction with the Au complex may be insufficient and weak, hence leading to aggregation to large Au particles without significant stabilization of Au species during the calcination at 673 K.

It is also to be noted that the sharpness of Au(111) diffraction line at $2\theta = 38.2^\circ$ for $\mathbf{1}/\mathrm{Fe_2O_3}$ was almost the same as that for $\mathbf{2}/\mathrm{Fe(OH)}_3^*$ (Figs. 3b and 3d), while the $\mathbf{2}/\mathrm{Fe(OH)}_3^*$ catalyst showed a much higher activity for the catalytic CO oxidation reaction than the $\mathbf{1}/\mathrm{Fe_2O_3}$ catalyst. The XRD patterns for the supports in the $\mathbf{1}/\mathrm{Fe_2O_3}$ and $\mathbf{2}/\mathrm{Fe(OH)}_3^*$ catalysts are different from each other. These results imply that the catalytic activity depends on not only the size of Au particles but also the nature of the support. It is evident that attaching the Au complexes on the as-precipitated metal hydroxides is superior to impregnating the Au complexes on the conventional metal oxides in preparation of small supported Au particles.

Thus it is suggested that the way to obtain highly dispersed Au particles active for the low-temperature CO oxidation is to choose suitable Au complexes as precursors which can be easily decomposed at mild temperatures and to prepare the as-precipitated metal hydroxides as precursors for oxide supports which have many surface OH groups reactive to the Au complexes, and to transform both precursors to Au particles and oxide supports under their chemical interaction by the temperature-programmed calcination in air.

Hoflund and co-workers claimed that some of Au is nonmetal and that this Au may be responsible for the low-temperature activity (18, 40). Haruta and co-workers reported that the sample having both metallic and nonmetallic Au species was not more active than the sample having only metallic Au species (10). Recently, it was suggested by XPS and ISS that the near-surface region of $\mathrm{Au/Fe_2O_3}$ contains more Au as compared with that of $\mathrm{Au/Co_3O_4}$, where Au is present as crystallites and small amounts of nonmetallic Au species are also present. Our XPS measurement provided no evidence on the presence of cationic Au species on the $\mathbf{1}/\mathrm{Fe(OH)}_3^*$ surface.

The structure of $TiO_2$ in $\mathbf{1}/\mathrm{Ti(OH)}_4^*$ was significantly affected by hydrolysis reagents used for preparation of the as-precipitated $\mathrm{Ti(OH)}_4^*$ as shown in Fig. 2. Two types of $TiO_2$, anatase and amorphous $TiO_2$, were formed by using *deionized* water and an aqueous solution of $Na_2CO_3$ as hydrolysis reagents, respectively. The $\mathbf{1}/\text{S-}\mathrm{Ti(OH)}_4^*$ (amorphous $TiO_2$) catalyst exhibits much higher activity for CO oxidation than the $\mathbf{1}/\text{W-}\mathrm{Ti(OH)}_4^*$ (anatase $TiO_2$) catalyst as shown in Fig. 6. Thus the presence of $Na^+$ ions gives profound effects on both the morphology and catalytic property of the oxide. Figure 2 also shows the effect of Na doping to the as-precipitated $\text{W-}\mathrm{Ti(OH)}_4^*$ on the morphology of the bulk and the size of Au particles. The anatase structure and the size of Au particles of $\mathbf{1}/\text{W-}\mathrm{Ti(OH)}_4^*$ were unchanged by the Na doping. On the other hand, the catalytic CO oxidation activity of $\mathbf{1}/\text{W-}\mathrm{Ti(OH)}_4^*$ was remarkably promoted by the Na doping to the $\text{W-}\mathrm{Ti(OH)}_4^*$ ($\mathbf{1}/\text{D-}\mathrm{Ti(OH)}_4^*$), as shown in Fig. 6. These results assume that small Au particles on the titanium oxides prepared by the $Na_2CO_3$ treatments, independent of amorphous and anatase forms, were very active for the low-temperature CO oxidation. The mechanism for enhancement of CO oxidation by $Na^+$ dope is not clear at present.

The steady-state catalytic performance of the Au samples was recorded without deactivation over 8 h time-on-stream in the present study. The activities of the catalysts, particularly containing basic supports like MgO, can vary over a long induction period as reported in the literature (25). In addition to the present results, further study on decay profile of the activity may be necessary for industrial application of the samples.

When the $Au(PPh_3)Cl/Fe(OH)_3^*$ catalyst was prepared and calcined in the similar manner to that for **1**/$Fe(OH)_3^*$, the XRD peak at 38.2° for Au(111) in Fig. 3e was sharp and intense, indicating the formation of the larger Au particles and consequently the catalytic activity of the $Au(PPh_3)Cl/Fe(OH)_3^*$ for CO oxidation was very low so that it was active only above 500 K as shown in Fig. 8. $Au(PPh_3)(NO_3)$ was heat-sensitive and $[Au_9(PPh_3)_8](NO_3)_3$ decomposed at 503 K, while $Au(PPh_3)Cl$ (mp.; 516–525 K) was stable around 570 K under air. The as-precipitated metal hydroxides are transformed to partially dehydrated metal oxides before the decomposition of $Au(PPh_3)Cl$. Under this situation the Cl-containing Au complex decomposes to Au metallic particles on metal oxide surface rather than metal hydroxide surface. The Au particle sizes in **2**/$Fe(OH)_3^*$ and $HAuCl_4/Fe(OH)_3^*$ are estimated to be similar and larger than 12 nm in Fig. 3. The former catalyst shows excellent catalysis for CO oxidation, whereas the latter catalyst shows negligible activity at the low temperatures. Thus the presence of Cl involved in the Au precursor not only increases the Au particle size but also suppresses catalytic CO oxidation at the surface, which agrees with the literature (17).

## CONCLUSION

The supported Au catalysts with small Au particles were prepared by attaching the Au phosphine complexes, $Au(PPh_3)(NO_3)$ (**1**) and $[Au_9(PPh_3)_8](NO_3)_3$ (**2**), on the wet as precipitated metal hydroxides, followed by the temperature-programmed decomposition and calcination in a flow of air. The obtained **1** and **2**/$M(OH)_x^*$ catalysts ($M = Mn^{2+}$, $Co^{2+}$, $Fe^{3+}$, $Ni^{2+}$, $Zn^{2+}$, $Mg^{2+}$, $Cu^{2+}$, and $Ti^{4+}$) are highly active for CO oxidation at low temperatures below 273 K compared to the corresponding Au/MxOy catalysts prepared by supporting **1** or **2** on conventional metal oxides. Such efficient catalysts were not obtained by supporting **1** or **2** on commercially available $M(OH)_x$ and water-exposed $M_xO_y$ followed by the similar calcination to that for the case of **1** or **2**/$M(OH)_4^*$. The Au particles in **1** or **2**/$M(OH)_x^*$ were estimated to be small, typically the size for **1**/$Fe(OH)_3^*$ being about 2.9 nm by EXAFS, XRD, and TEM. The reactivity of the catalysts for CO oxidation is positively affected by sodium cation, whereas negatively affected by chloride ion. Sodium cations and chloride anions have significant effects on Au particle size and support morphology. The catalysts derived from **1** are more active for CO oxidation than those derived from **2**.

## ACKNOWLEDGMENT

This work has been supported by CREST (Core Research for Evolutional Science and Technology) of Japan Science and Technology Corporation (JST).

## REFERENCES

1. Stark, D. S., Crocker, A., and Steward, G. J., *J. Phys. E: Sci. Instrum.* **16**, 158 (1983).
2. Stark, D. S., and Harris, M. R., *J. Phys. E: Sci. Instrum.* **16**, 492 (1983).
3. Stark, D. S., and Harris, M. R., *J. Phys. E: Sci. Instrum.* **21**, 715 (1988).
4. Schryer, D. R., Upchurch, B. T., van Norman, J. D., Brown, K. G., and Schryer, J., *J. Catal.* **122**, 193 (1990).
5. Fuller, M. J., and Warwick, M. E., *J. Catal.* **34**, 445 (1974).
6. Bond, G. C., Molloy, L. R., and Fuller, M. J., *J. Chem. Soc. Chem. Commun.*, 796 (1975).
7. Croft, G., and Fuller, M. J., *Nature* **269**, 585 (1977).
8. Haruta, M., Kobayashi, T., Sano, H., and Yamada, N., *Chem. Lett.*, 405 (1987).
9. Haruta, M., Yamada, N., Kobayashi, T., and Iijima, S., *J. Catal.* **115**, 301 (1989).
10. Haruta, M., Tsubota, S., Kobayashi, T., Kageyama, H., Genet, M. J., and Delmon, B., *J. Catal.* **144**, 175 (1993).
11. Tsubota, S., Ueda, A., Sakurai, H., Kobayashi, T., and Haruta, M., *ACS. Symp. Ser.* **552**, 420 (1994).
12. Boccuzi, T., Tsubota, S., and Haruta, M., *J. Elec. Spectrosc. Relat. Phenom.* **64/65**, 241 (1993).
13. Haruta, M., Tsubota, S., Kobayashi, T., Ueda, A., Sakurai, H., and Ando, M., *Stud. Surf. Sci. Catal.* **75**, 2657 (1993).
14. Gardner, S. D., Hoflund, G. B., Davidson, M. R., and Schryer, D. R., *J. Catal.* **115**, 132 (1989).
15. Gardner, S. D., Hoflund, G. B., Schryer, D. R., and Upchurch, B. T., *J. Phys. Chem.* **95**, 835 (1991).
16. Schryer, D. R., Upchurch, B. T., Sidney, B. D., Brown, K. G., Hoflund, G. B., and Herz, R. K., *J. Catal.* **130**, 314 (1991).
17. Gardner, S. D., Hoflund, G. B., Schyer, D. R., Schryer, J., Upchurch, B. T., and Kielin, E. J., *Langmuir* **7**, 2135 (1991).
18. Gardner, S. D., Hoflund, G. B., Davidson, M. R., Laitinen, H. A., Schryer, D. R., and Upchurch, B. T., *Langmuir* **7**, 2140 (1991).
19. Hoflund, C. B., Gardner, S. D., Schryer, D. R., Upchurch, B. T., and Kielin, E. J., *Appl. Catal. B: Environmental* **6**, 117 (1995).
20. Imamura, S., Sawada, H., Uemura, K., and Ishida, S., *J. Catal.* **109**, 198 (1988).
21. Imamura, S., Yoshie, S., and Ono, Y., *J. Catal.* **115**, 258 (1989).
22. Lin, S. D., Bollinger, M., and Vannice, M. A., *Catal. Lett.* **17**, 245 (1993).
23. Knell, A., Barnickel, P., Baiker, A., and Wokaun, A., *J. Catal.* **137**, 306 (1992).
24. Baiker, A., Maciejewski, M., Tagliaferri, S., and Hug, P., *J. Catal.* **151**, 407 (1995).
25. Srinivas, G., Wright, J., Bai, C.-S., and Cook, R., *Stud. Surf. Sci. Catal.* **101**, 427 (1996).
26. Bond, G. C., and Sermon, P. A., *Gold Bull.* **6**, 102 (1973).
27. Yermakov, Y. I., Kuznetsov, B. N., and Zakharov, V. A., "Catalysis by Supported Complexes." Elsevier, Amsterdam, 1981.
28. Basset, J. M., *J. Mol. Catal.* **21**, 95 (1983).
29. Iwasawa, Y., Ed., "Tailored Metal Catalysts," Reidel, Amsterdam, 1986.
30. Maire, G., *Stud. Surf. Sci., Catal.* **29**, 509 (1986).

31. Gates, B. C., *Chem. Rev.* **95**, 511 (1995).
32. Iwasawa, Y., *in* "Proceedings, 11th International Congress on Catalysis, Baltimore, 1996)," p. 21. Studies in Surface Science and Catalysis, Vol. 101.
33. Yuan, Y., Asakura, K., Wan, H., Tsai, K., and Iwasawa, Y., *Chem. Lett.*, 129 (1996).
34. Yuan, Y., Asakura, K., Wan, H., Tsai, K., and Iwasawa, Y., *Catal. Lett.*, in press.
35. Yuan, Y., Asakura, K., Wan, H., Tsai, K., and Iwasawa, Y., *Chem. Lett.*, 755 (1996).
36. Mueting, A. M., Alexander, B. D., Boyle, P. D., Casalnuovo, A. L., Ito, L. N., Johnson, B. J., and Pignolet, L. H., *in* "Inorganic Syntheses" (R. N. Grimes, Ed.), Vol. 29, p. 280. Wiley, New York, 1992.
37. Cariati, F., and Naldini, L., *J. C. S. Dalton*, 2286 (1972).
38. Rehr, J. J., Mustre, de L. J., Zabinsky, S. I., and Albers, R. C., *J. Am. Chem. Soc.* **113**, 5235 (1991).
39. Iwasawa, Y., Ed., "X-Ray Absorption Fine Structure for Catalysts and Surfaces." World Scientific, Singapore, 1996.
40. Epling, W. S., Hoflund, G. B., Weaver, J. F., Tsubota, S., and Haruta, M., *J. Phys. Chem.* **100**, 9929 (1996).